Supporting Information

Alkali Metal Intercalation and Rapid Exfoliation of Two-Dimensional Fullerene Frameworks

Xin Yuan[a], Yan Xu[b], Zhicong Hu[a], Guanglin Huang*[a], Jinwei Zhang[a], Yisheng Wei[a], Haohan Wang[a], Yusheng Lu[a], Shuwen Jia[a], Chenli Huang[a], Kun Guo[a], Lei Shi*[b], Xing Lu[a] & Lipiao Bao*[a]

---

[a]State Key Laboratory of Materials Processing and Die & Mould Technology, School of Materials Science and Engineering

Huazhong University of Science and Technology

1037, Luoyu Road, Wuhan 430074, P. R. China

E-mail: baol@hust.edu.cn; guanglinhuang@hust.edu.cn

[b]State Key Laboratory of Optoelectronic Materials and Technologies, Guangdong Basic Research Center of Excellence for Functional Molecular Engineering, Nanotechnology Research Center, School of Materials Science and Engineering

Sun Yat-sen University

Guangzhou 510275, P. R. China

E-mail: shilei26@mail.sysu.edu.cn

Keywords: fullerene framework; alkali-metal intercalation; *in-situ* Raman spectroscopy; rapid exfoliation; 2D-C_{60}

Contents

1. Materials

Fullerene (C_{60}, 99.5%), magnesium powder (Mg, 99.5%), Tetrahydrofuran (99.9%, extra dry with molecular sieves), Benzonitrile (PhCN, 99%, extra Dry with molecular sieves), Metal sodium/potassium (Na/K, 99.99%) and Cyclohexane (CYH, 99.0%) were purchased from Funano, Aldrich, Innochem, Energy chemical, Alfa-Aesar, Sinopharm Chemical Reagent Co., Ltd., respectively, and used without further purification.

2. Equipment

The morphology and topography of the samples were investigated using a Zeiss Sigma 300 field-emission scanning electron microscope (SEM), an Oxford Instruments Jupiter XR atomic force microscope (AFM). The structural characteristics of the samples were characterized using and a JEOL JEM-ARM200F field-emission transmission electron microscope (TEM) and X-ray diffraction (XRD) data were collected using a PANalytical B.V. Empyrean X-ray diffractometer with Cu-Kα radiation. To obtain optical features, Raman spectra were recorded on a TriVista557 Raman microscope equipped with a 561 nm excitation laser.

3. Synthesis of Mg_4C_{60} crystals

Using the reported chemical vapor transport technology (CVT, Figure S1a),[S1–S3] C_{60} powder (60 mg) and magnesium powder (30 mg) were mixed uniformly and sealed in a quartz tube, placed in a two-zone furnace at 600-500 ^{o}C for 24 hours, and the heating rate was set at 5 ^{o}C/min. The end containing C_{60} and magnesium powder is placed in the high temperature zone, and Mg_4C_{60} crystals are collected in the low temperature zone. The final product (Figure S1b) is collected and stored in an argon-filled glove box. Hexagonal structures on the front side of the crystal were observed by optical microscopy (OM), revealing lateral dimensions of approximately 100 μm (Figure S1c). The scanning electron microscopy (SEM) image (Figure S2d) further elucidates the layered hexagonal morphology of the crystal, which is consistent with the OM findings

and aligns with the characteristic structural features of the hexagonal phase Mg_4C_{60} crystal. The X-ray pattern of these crystals (Figure S1e) matches well with the pattern extracted from the single-crystal diffraction data of Mg_4C_{60} in literature.[S2] The Raman spectra image of Mg_4C_{60} single crystals (Figure S1f) is consistent with the literature reports.[S2] Therefore, the synthesized material is conclusively identified as single-crystalline quasi-two-dimensional polymeric fullerene Mg_4C_{60}.

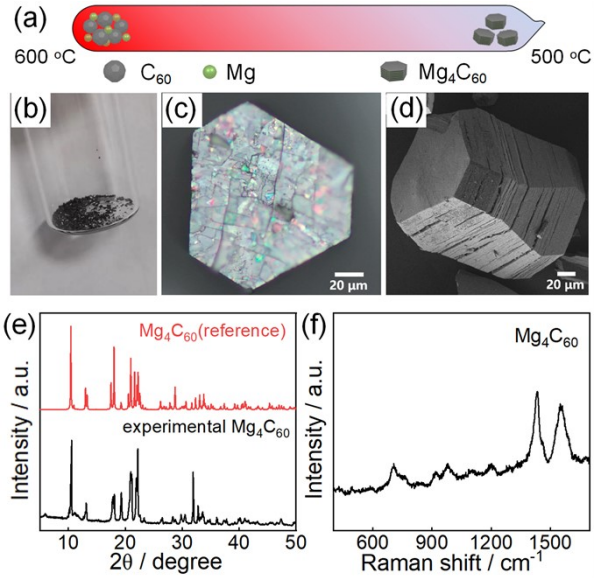

Figure S1. (a) Schematic of the CVT technique used for the growth of Mg_4C_{60} single crystals; (b) Photograph, (c) optical micrograph and (d) SEM image of Mg_4C_{60} single crystals; (e) XRD spectra of Mg_4C_{60} single crystals; (f) Raman spectra of Mg_4C_{60} single crystals.

4. Alkali metal intercalation in Mg_4C_{60} crystals

The Mg_4C_{60} crystals are vacuum-sealed with an excess amount of sodium/potassium metal in a quartz tube in the glove box to remove the oxides on the surface of sodium or potassium. The quartz tube with an optical an observation window for *in-situ* Raman monitoring was then placed under our Raman setup with a home-built heating system. The temperature difference between the alkali-metal side and the Mg_4C_{60} side was set as 50 °C. The intercalated compound K/Na-Mg_4C_{60} can also be obtained by directly mixing Mg_4C_{60} crystals with sodium/potassium in a glass vial at 110 °C under inert conditions. In this process, the sodium/potassium metal melts and penetrates into the

Mg_4C_{60} crystal layers, so a lower temperature than the gas-phase synthesis method is used.

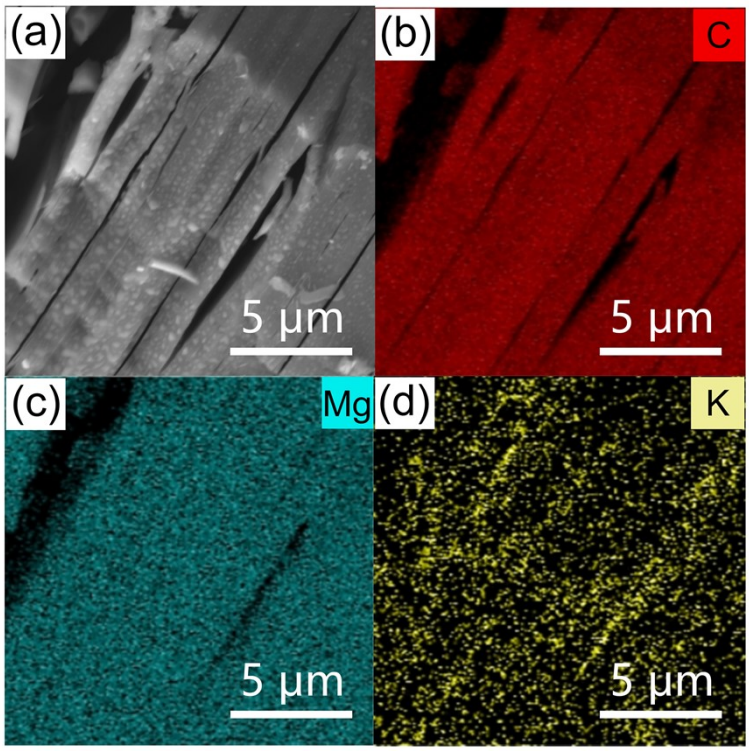

Figure S2. The SEM image and EDX mapping of K-Mg_4C_{60}-400. Acceleration voltage: 10 kV.

Table S1. The EDX mapping of K-Mg_4C_{60}-400.

Element	Line type	Wt%	Wt % Sigma	At%
C	K	89.93	0.07	95.07
Mg	K	8.41	0.06	4.39
K	K	1.67	0.05	0.54
Total		100.00		100.00

5. Detection of Mg^{2+} using Titan Yellow solution

Preparation of Titan Yellow solution[S4] 0.1 g of Titan Yellow ($C_{28}H_{19}N_5Na_2O_6S_4$) was completely dissolved in 100 mL distilled water (slight heating may be used to aid dissolution). The pH value of this solution was set to > 10 (alkaline environment) with the addition of suitable NaOH solution. To enhance the colour development, a small amount of PVA (0.1%) can be added to increase the viscosity of the solution. The solution will change from yellow to red or reddish-brown precipitate upon the complexation with Mg^{2+}.

A small aliquot of K-intercalated Mg_4C_{60} (K-Mg_4C_{60}) was dispersed in toluene and left undisturbed for three days. Nearly the entire solid remained insoluble, while only trace amounts of dissociated C_{60} dissolved, imparting a pale-violet hue to the solution (Figure S3). This outcome indicates that Mg_4C_{60} undergoes negligible cleavage during the intercalation process and thus substantiates the successful insertion of K^+ ions. To probe possible magnesium leaching, K-Mg_4C_{60}-400 was treated with the prepared Titan Yellow solution (Figure S3); no Mg^{2+} signal was detected on the sample surface. Likewise, Mg^{2+} detection of the glass tube employed for synthesizing K-Mg_4C_{60}-400 (Figure S4a) revealed no Mg^{2+} absorbed on the glass wall. Energy-dispersive X-ray (EDX) analysis of the tube's inner wall (Figure S4b, Table S2) also showed no Mg^{2+} signal. These results confirm that magnesium remains firmly embedded and is not extruded during K intercalation. For further verification, elemental Mg and K were each vacuum-sealed in separate glass tubes and heated to 400 ^oC (Figure S4c). Only the tube containing K exhibited sublimation and developed a brown-yellow coloration, whereas the Mg-containing tube showed no such change. This experiment corroborates that, at 400 ^oC, potassium can intercalate into Mg_4C_{60} while magnesium remains securely in place without deintercalation.

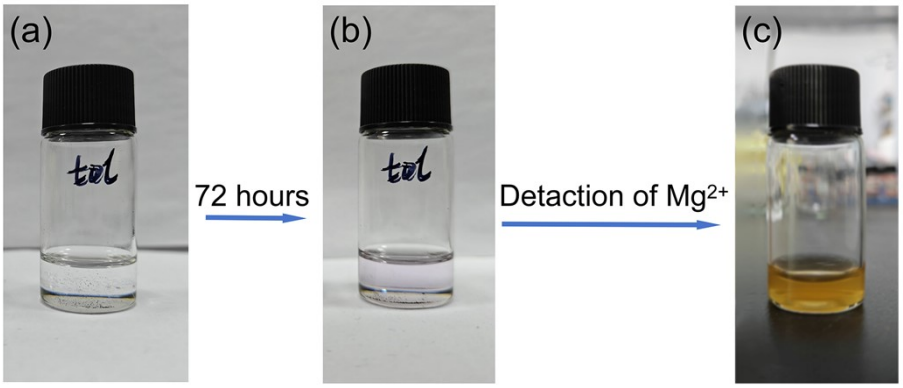

Figure S3. Photographs of K-Mg_4C_{60}-400 (a-b) in toluene and (c) solution containing titan yellow solution.

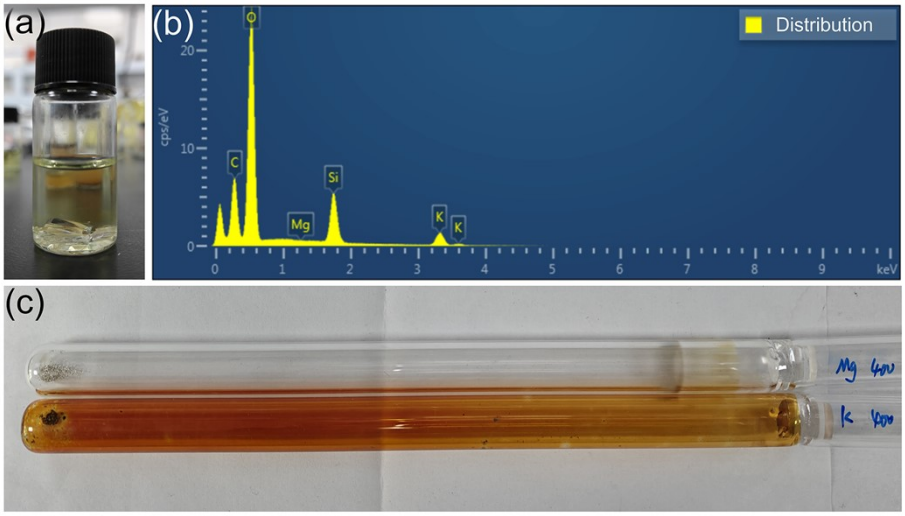

Figure S4. (a) Photograph of the glass tube of K-Mg_4C_{60}-400 in solution containing Titan Yellow solution, (b)The SEM-EDX analysis of the glass tube of K-Mg_4C_{60}-400, (c) Photograph of the glass tube of Mg or K after 400 ^oC thermal treatment.

Table S2. The SEM mapping of the inner wall of the glass tube of K-Mg_4C_{60}-400.

Element	Line type	Wt%	Wt % Sigma	At%
C	K	25.95	0.48	34.23
Mg	K	0.00	0.04	0.00
K	K	6.21	0.11	2.52
Si	K	9.20	0.10	5.19
O	K	58.63	0.40	58.06
Total		100.00		100.00

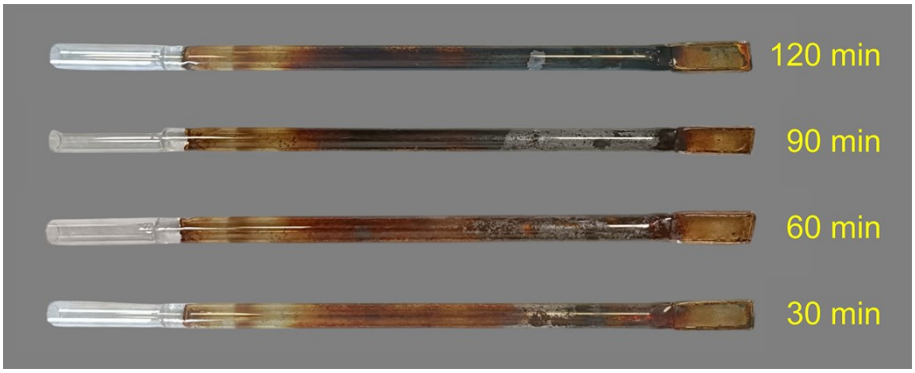

Figure S5. (a) Photograph of the glass tube of K-Mg_4C_{60} after different intercalation times at 400 °C.

6. Rapid Exfoliation of Mg_4C_{60}

In a stirring 2M benzonitrile solution in THF, K/Na-Mg_4C_{60} was added and the solution intermediately changed from colorless to red. This significant color change suggests the formation of benzonitrile anions and the electron-extraction from the intercalation compounds. In the meantime, massive exfoliated flakes of 2D-C_{60} can be observed in the solution. The solution was then under further stirring for a few minutes. Alternatively, tip-sonication will remarkably accelerate the process to a time of 3 min. The ultrasonic energy helps promote further exfoliation of the K/Na-Mg_4C_{60} layers and the formation of 2D-C_{60}.

To obtain solids of exfoliated 2D-C_{60}, cyclohexane, THF, and deionized water was added to the dispersion to wash-up. After settling, layer separation occurred, the middle layer was collected and washed multiple times with THF, ethanol, or deionized water to remove residual potassium and solvent. The sample was subjected to freeze-drying for 24 hours to avoid aggregation. The obtained 2D-C_{60} solid can be re-dispersed in an inert solvent (ethanol, THF, NMP etc).

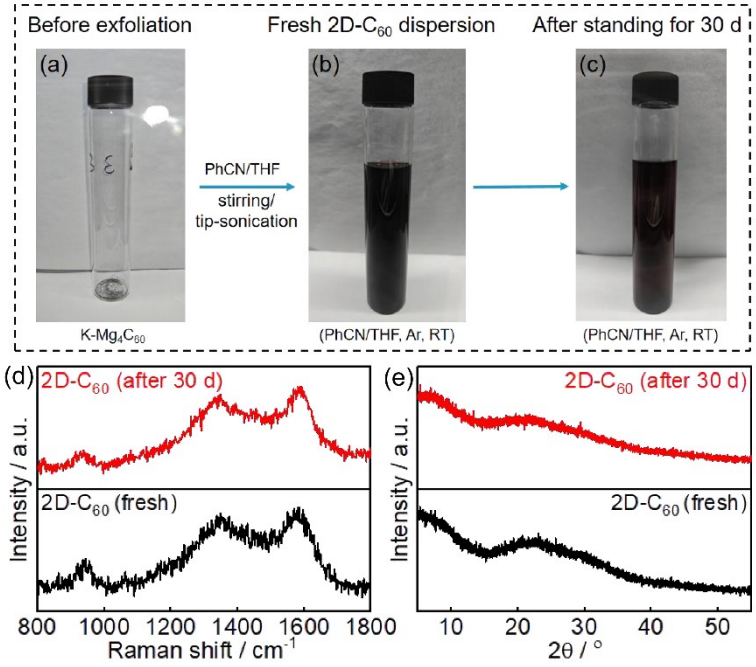

Figure S6. Photographs illustrating benzonitrile-driven exfoliation and stability of 2D-C_{60}. (a) Vial containing K-Mg_4C_{60} powder before exfoliation. (b) Freshly prepared 2D-C_{60} dispersion obtained by adding a PhCN/THF mixture to K-Mg_4C_{60} followed by stirring or tip-sonication under Ar at room temperature. (c) The same 2D-C_{60} dispersion after standing for 30 days under Ar at room temperature, showing no obvious precipitation, indicative of good macroscopic stability. (d) Raman spectra and (e) XRD patterns of exfoliated 2D-C_{60} samples collected from the fresh dispersion (black) and from the dispersion after 30 days (red). The essentially unchanged Raman and XRD features confirm that the 2D-C_{60} framework remains structurally stable upon long-term storage of the dispersion.

When the K/Na-intercalated Mg_4C_{60} framework is brought into contact with liquid benzonitrile (PhCN), a heterogeneous electron-transfer process is initiated at the solid–liquid interface, closely analogous to the discharge of KC_8 and other K-intercalated carbons in PhCN. In our stage-I $A_xMg_4C_{60}$ intermediates (A = K, Na; x ≈ 3), the A2 g mode of C_{60} is red-shifted by ≈16 cm^{-1} relative to neutral C_{60}, which, using the widely adopted calibration of ≈6-7 cm^{-1} per electron, corresponds to roughly 2-3 extra electrons per C_{60} cage. After quenching and exfoliation, the A2 g frequency of 2D-C_{60} lies much closer to that of a neutral polymeric framework, implying that only a small fraction (≤ 0.3-0.5 e^- per C_{60}) of the original excess charge remains. Thus, the majority of electrons initially supplied by K/Na are transferred to PhCN (and possibly to the co-solvent), generating $PhCN^{\bullet-}$ species in solution and partially oxidising the fulleride framework.

The interfacial electron transfer is tightly coupled to cation extraction and solvent co-intercalation. As $A_xMg_4C_{60}$ is oxidized, the compensating K^+/Na^+ (and to a lesser extent Mg^{2+}) cations become destabilized in the interlayer galleries and are strongly solvated by the polar aprotic PhCN/THF mixture. These solvated cations migrate into the liquid phase, effectively removing the ionic “glue” that held the negatively charged C_{60} sheets together. At the same time, PhCN molecules penetrate between adjacent 2D-C_{60} sheets, further expanding the interlayer spacing and weakening interlayer interactions. Under mild agitation, this combination of charge neutralization, cation deintercalation and solvent insertion allows the layered Mg_4C_{60} framework to delaminate rapidly into mono- and bilayer 2D-C_{60} flakes, as schematically illustrated in Figure S7.

These observations also rationalize why benzonitrile is particularly effective as a quenching solvent. PhCN has a sufficiently positive reduction potential to accept electrons from strongly reduced fullerides while preserving the carbon framework, provides good solvation for K^+/Na^+ cations as a polar aprotic solvent, and exhibits low nucleophilicity so that it primarily engages in outer-sphere redox rather than covalent addition to the C_{60} cages. Taken together, these properties allow PhCN to act

simultaneously as an electron acceptor, a cation-solvating medium and a co-intercalating spacer, enabling a rapid and chemically gentle route from $A_xMg_4C_{60}$ to metal-free 2D-C_{60} sheets.

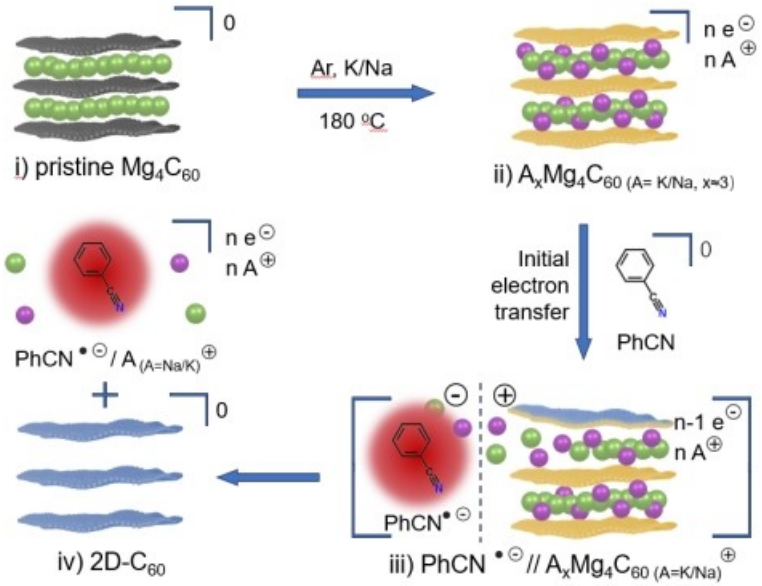

Figure S7. Schematic illustration of the alkali-metal intercalation and benzonitrile-driven exfoliation of Mg_4C_{60}. (i) Pristine Mg_4C_{60} consisting of covalently linked 2D-C_{60} sheets (grey) and interlayer Mg^{2+} pillars (green). (ii) Formation of highly reduced $A_xMg_4C_{60}$ (A = K/Na, $x \approx 3$) by vapour-phase K/Na intercalation at 180 °C, where alkali cations (purple) occupy the interlayer spaces and donate electrons to the C_{60} framework. (iii) Upon contact with benzonitrile (PhCN), interfacial electron transfer from $A_xMg_4C_{60}$ to PhCN generates $PhCN^{\cdot -}$, accompanied by deintercalation/solvation of A^+ and partial oxidation of the fulleride framework. (iv) Loss of the ionic "pillars", together with solvent co-intercalation, leads to delamination of the layered framework into charge-neutral mono- and bilayer 2D-C_{60} sheets.

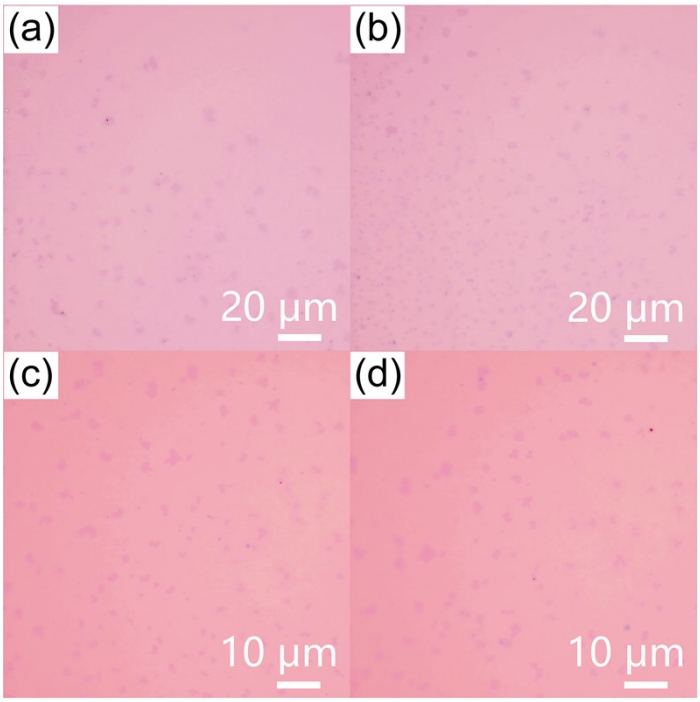

Figure S8. Optical images of the exfoliated 2D-C_{60} on a SiO_2/Si substrate.

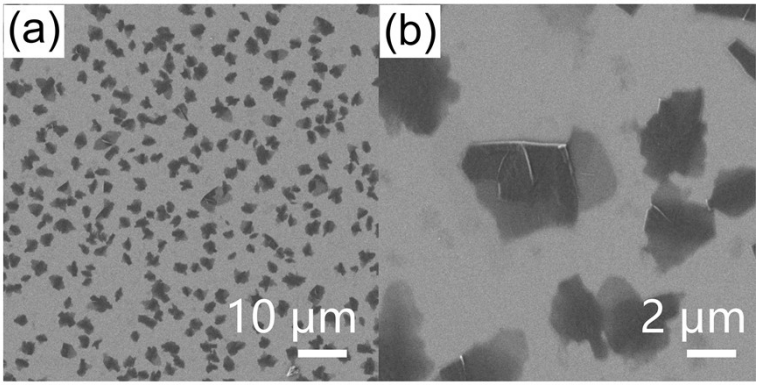

Figure S9. Scanning electron microscopic (SEM) images of the exfoliated 2D-C_{60}.

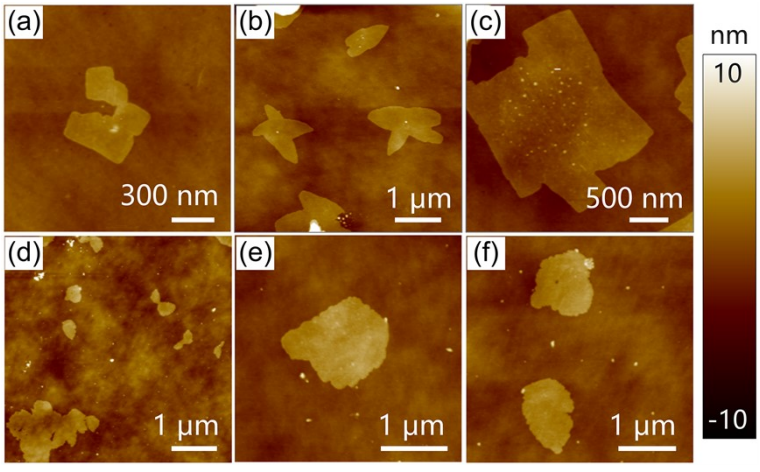

Figure S10. AFM image of the exfoliated 2D-C_{60} showing mono-/bi-layer nature.

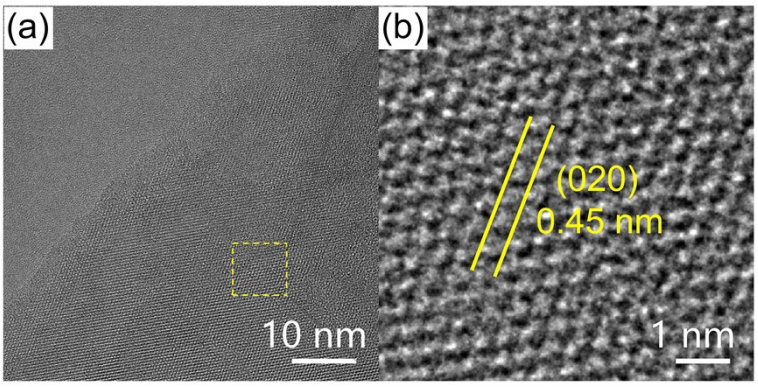

Figure S11. TEM images of the exfoliated 2D-C_{60} using our rapid exfoliation method.

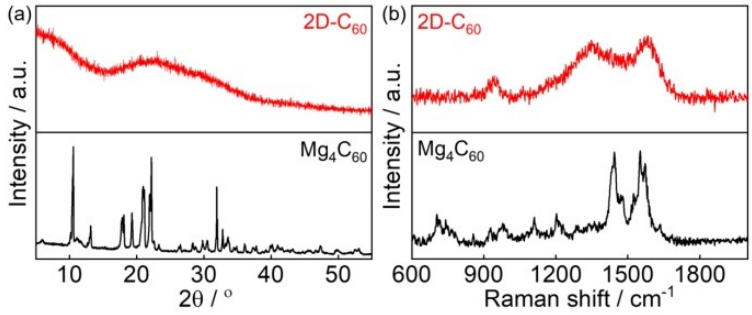

Figure S12. (a) XRD patterns and (b) Raman spectra of bulk Mg_4C_{60} (bottom, black) and exfoliated 2D-C_{60} films (top, red) on Si/SiO_2 substrates. The sharp Bragg reflections of crystalline Mg_4C_{60} disappear after benzonitrile quenching and exfoliation, and are replaced by a broad amorphous-like halo for 2D-C_{60}. Likewise, the well-resolved fulleride Raman modes of Mg_4C_{60} evolve into broadened bands centred near the neutral polymeric-C_{60} region, indicating the loss of the Mg-pillar framework and the formation of a largely metal-free 2D-C_{60} network.

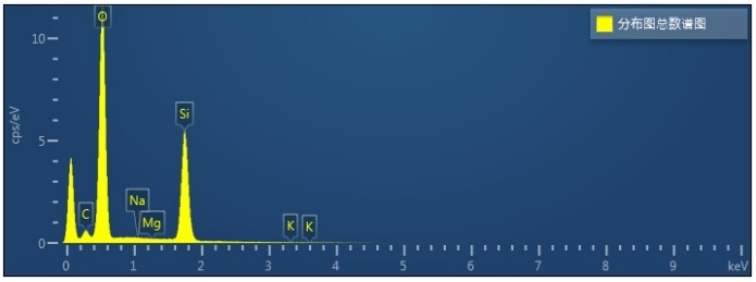

Figure S13. SEM-EDX spectrum of an exfoliated 2D-C_{60} flake on a Si/SiO_2 support. Besides the strong signals from C and O (2D-C_{60} and surface adsorbates) and Si from the substrate, only very weak Na, Mg and K signals are detected, close to the instrumental detection/quantification limit, indicating that alkali and alkaline-earth metals are present, if at all, only at trace levels in the exfoliated sheets.

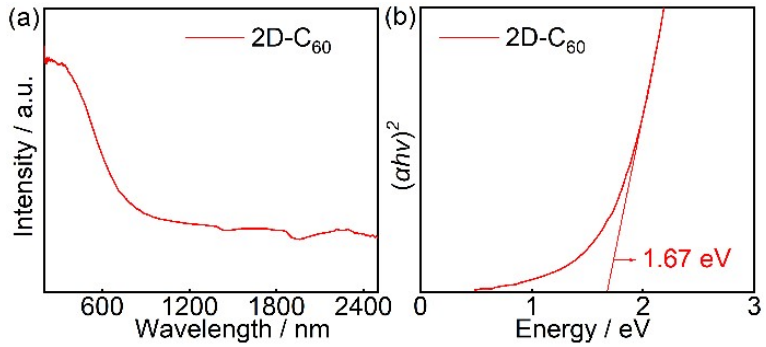

Figure S14. (a) UV–vis–NIR absorption spectrum of 2D-C_{60}. (b) Tauc plot $(\alpha h\nu)^2$ vs photon energy for a direct transition; linear extrapolation gives an optical gap of 1.67 eV.

References:

S1 E. Meirzadeh, A. M. Evans, M. Rezaee, M. Milich, C. J. Dionne, T. P. Darlington, S. T. Bao, A. K. Bartholomew, T. Handa, D. J. Rizzo, R. A. Wiscons, M. Reza, A. Zangiabadi, N. Fardian-Melamed, A. C. Crowther, P. J. Schuck, D. N. Basov, X. Zhu, A. Giri, P. E. Hopkins, P. Kim, M. L. Steigerwald, J. Yang, C. Nuckolls and X. Roy, *Nature*, 2023, **613**, 71-76.

S2 L. Hou, X. Cui, B. Guan, S. Wang, R. Li, Y. Liu, D. Zhu and J. Zheng, *Nature*, 2022, **606**, 507-510.

S3 M. Tanaka and S. Yamanaka, *Cryst. Growth Des.*, 2018, **18**, 3877-3882.

S4 A. Shokrollahi, K. Hemmatidoust and F. Zarghampour, *J. Taibah Univ. Sci.*, 2016, **10**, 161-167.